

Robust Retinal Vessel Segmentation from a Data Augmentation Perspective

Xu Sun, Xingxing Cao, Yehui Yang, Lei Wang, and Yanwu Xu*

Baidu Inc., Beijing, China.

* Corresponding author, xuyanwu@baidu.com

Abstract. Retinal vessel segmentation is a fundamental step in screening, diagnosis, and treatment of various cardiovascular and ophthalmic diseases. Robustness is one of the most critical requirements for practical utilization, since the test images may be captured using different fundus cameras, or be affected by various pathological changes. We investigate this problem from a data augmentation perspective, with the merits of no additional training data or inference time. In this paper, we propose two new data augmentation modules, namely, channel-wise random Gamma correction and channel-wise random vessel augmentation. Given a training color fundus image, the former applies random gamma correction on each color channel of the entire image, while the latter intentionally enhances or decreases only the fine-grained blood vessel regions using morphological transformations. With the additional training samples generated by applying these two modules sequentially, a model could learn more invariant and discriminating features against both global and local disturbances. Experimental results on both real-world and synthetic datasets demonstrate that our method can improve the performance and robustness of a classic convolutional neural network architecture. Source codes are available here.

Keywords: Robust retinal vessel segmentation · Data augmentation.

1 Introduction

Retinal vessel segmentation plays a crucial role in computer-aided screening, diagnosis, and treatment of various cardiovascular and ophthalmic diseases such as stroke, diabetics, hypertension and retinopathy of prematurity [10]. A substantial amount of work has been reported in the last two decades for automated detecting blood vessels in retinal fundus images. These algorithms can mainly be categorized into two groups: the unsupervised and supervised methods. The unsupervised methods rely on strong but intuitive priors of the blood vessel appearance [2,3], while the supervised methods utilize labelled datasets based on given features [4,15]. Among these algorithms, supervised segmentation of blood vessels based on deep learning has reached new performance levels [1,5,19].

Despite architectural advances based on deep learning have led to enormous progress at segmenting vessels in curated datasets, their ability to generalize to

new situations is rarely studied. In contrast, the generalization ability, which refers to robustness, is an important factor for algorithms performance. To improve robustness, there exist two issues which need special attention. First, in the real world context of retinal fundus image analysis, the input images may come from different kinds of digital fundus camera systems. Since the tonal quality of a fundus image is affected by the characteristics of these systems [17], models fitting well to datasets collected from a specific class of fundus camera might fail to generalize to those captured from other types of machines. Second, for retinal vessel segmentation models to be adopted in practice, they also need to be robust on pathological changes, especially on those not included during the training stage.

These issues can be alleviated by different strategies. For instance, image pre-processing techniques like contrast limited adaptive histogram equalization try to decrease the difference among samples by redistributing their pixel values. However, they only lead to limited improvement yet require additional inference time. Domain adaptation [9,21], on the other hand, learns to adapt models between domains. But it needs additional data from the target domain to retrain the models when deploying to a new circumstance. In contrast, data augmentation methods, which includes input transforms that the model should be invariant against, show great merits of without requiring any extra training data or inference time. Motivated by that, in this paper we investigate the robust retinal vessel segmentation problem from a data augmentation perspective.

Our method consists of two novel data augmentation modules, *i.e.*, channel-wise random gamma correction and channel-wise random vessel augmentation, for training robust retinal vessel segmentation models. The former aims at varying the tonal quality of the entire image, while the latter mainly focuses on augmenting the visual appearance of retinal vessels. With the generated virtual training samples, a model is able to learn more representative features regardless of both global and local variations. The experimental results on three real world datasets suggest that the proposed method significantly increases the robustness on samples that are captured by different camera systems and/or affected by diverse pathological changes. Furthermore, we also construct a thorough set of synthetic images to demonstrate that models trained with our method are less sensitive to the variations of image brightness, contrast and saturation.

2 Methodology

In this section, we present a novel scheme to improve the robustness of retinal vessel segmentation, which comprises two data augmentation modules that increase the global and local invariance, respectively. Fig. 1 illustrates the process of virtual sample generation through the proposed data augmentation method.

2.1 Channel-wise Random Gamma Correction (CWRGC)

Gamma correction is a nonlinear operation used to encode and decode luminance or tristimulus values, and has been widely used as a image preprocessing step in

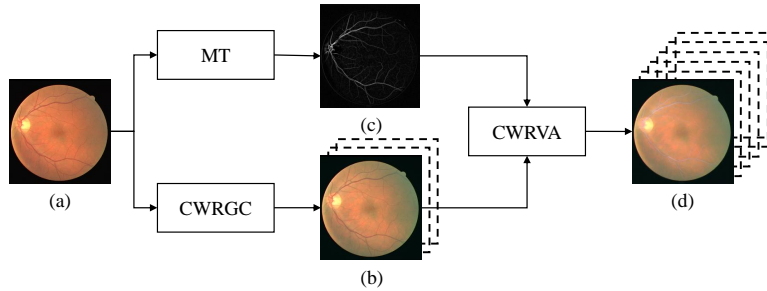


Fig. 1. Illustration of the proposed data augmentation scheme. (a) Original image from the DRIVE [16] training set. (b) Sample image augmented via channel-wise random gamma correction (CWRGC). (c) A rough vessel map generated by morphological transformation (MT). (d) sample images generated by additional channel-wise random vessel augmentation (CWRVA) on top of CWRGC.

automated vessel segmentation systems. Unlike current approaches which employ gamma correction in the HSV (Hue, Saturation, value) color space [12,20], we suggest to apply it directly in the RGB (Red, Green, Blue) color space. In particular, a simple yet effective data augmentation technique, termed channel-wise random gamma correction, is developed. This method is formulated as

$$\widehat{V}_i = V_i^{\gamma_i} \quad (1)$$

where \widehat{V}_i and V_i represent the intensity of the image before and after transformation, respectively. $\gamma_i > 0$ is the correction value, and subscript $i \in \{R, G, B\}$ denotes the corresponding red, green, or blue channel. By varying γ_i randomly, virtual examples covering a wide range of tonal quality can be created at the training stage. Fig. 1 (b) shows one of the generated images,

2.2 Channel-wise Random Vessel Augmentation (CWRVA)

Different from the first method that transforms the entire fundus images, our second method mainly focuses on blood vessel regions. This can be achieved by taking advantages of existing unsupervised methods, as they are able to provide the rough vessel maps without requiring annotations. To be specific, morphological transformation [11] is used here due to its simplicity of implementation and effectiveness in practice. When the structuring element used in the morphological opening is orthogonal to the vessel direction and longer than the vessel width, it will eradicate a vessel or part of it. Based on this observation, morphological transformation is defined as follows

$$I_{\text{th}}^\theta = I - (I \circ S_e^\theta), \quad (2)$$

$$I_{S_{\text{th}}} = \sum_{\theta \in A} I_{\text{th}}^\theta \quad (3)$$

where I_{th}^θ is the top-hat transformed image, I is the image to be processed, \circ is the opening operation, S_e is the structuring element, and $\theta \in \mathcal{A}$ is the angular rotation equally distributed in $[0, \pi)$.

Given the top-hat transformed image, the blood vessel attention map for each color channel of the fundus image can then be obtained by

$$M_i = \mathbb{N}(I_{S_{\text{th}}}) \cdot \lambda_i \quad (4)$$

where $\mathbb{N}(\mathbf{x})$ is a normalization function which scales and shifts the input array \mathbf{x} so that the minimum and maximum value of \mathbf{x} are 0 and 1, respectively, and $\lambda_i \in [0, 1]$ is a random decay coefficient with $i \in \{\text{R}, \text{G}, \text{B}\}$.

The proposed channel-wise random vessel augmentation is formulated as

$$\tilde{V}_i = V_i \cdot (1 - M_i) + M_i \cdot \mathcal{A} \quad (5)$$

where V_i and \tilde{V}_i denote the intensity values of the image before and after vessel augmentation, respectively, and $\mathcal{A} \in [0, 255]$ is the random disturbing intensity. Virtual images with various visual effect can be generated through changing λ_i in equation (4). A typical example is shown in Fig. 1 (d).

3 Experiments

To evaluate the effectiveness of our method, a thorough set of ablation study experiments are conducted. The first experiment is performed on three real world datasets to show how our method impacts robustness on testing images collected by a different fundus camera and/or affected by different pathological changes. Furthermore, we also utilize synthetic datasets to investigate the sensitivity of different models to the variations of image brightness, contrast and saturation.

3.1 Experiments Setup

We adopt the U-Net architecture [14] in our experiments due to its popularity in medical image analysis community and formation of the basis for most of the recent architectural advances at segmenting retinal vessels [6,18]. In particular, we replace its feature encoder module with the pretrained ResNet-50, remaining the first five feature extraction blocks without the global averaging pooling layer and the fully connected layers.

We employ random horizontal flip and random vertical flip with a probability of 50% as the basic data augmentation strategy (BS). In addition, two commonly used randomized data augmentation methods in literature are also implemented for comparison:

- RGN: Disturb the intensity of the red, green and blue channels by adding Gaussian noise with mean of 0 and standard deviation of 20.
- SVGC: Gamma correction of Saturation and Value (of the HSV color space) by raising pixels to a power in $[0.25, 4]$.

In our experiments, γ_i in equation (1) for the channel-wise random gamma correction (CWRGC) is randomly selected from $[0.33, 3]$, and λ_i in equation (4) for the channel-wise random vessel augmentation (CWRVA) is randomly picked in $[0, 1]$. All the models are trained on the DRIVE [16] training set using a publicly available library¹. We use the “step-scaling” method provided in the library to resize the input images to 640×640 , setting the scaling factor range from 0.75 to 1.25 with a step of 0.25. We use adam as the optimizer. The learning rate is initially set to be 0.005 and then decays following the “poly” policy with a power of 0.9. Instead of training all parameters from scratch, we fine-tune the network end-to-end from an ImageNet pre-trained model. We integrate both dice loss and binary cross entropy loss to train all models for 3000 epoches.

Following previous work, the retinal vessel segmentation results are evaluated quantitatively by the area under the receiver operation characteristic curve (AUC), accuracy (ACC), specificity (SP), sensitivity (SE), and F1-score (F1). However, we mainly focus on AUC and F1 when comparing the performance of different methods as they are more reliable for evaluating binary classifiers (say, to classify if a pixel belongs to vessels or not) [8]. In particular, when we conclude that one method outperforms another, we mean that it achieves both the higher AUC and F1 if without stating which metrics are used.

3.2 Generalization Across Different Datasets

To validate how our augmentations impact robustness in a realistic setting, models trained on the DRIVE training set are applied to three real world datasets:

- **Testing set of DRIVE** [16]: the fundus images are captured from the same digital fundus camera system as the training set.
- **Full set of STARE** [7]: this dataset is collected from a different type of fundus camera, and includes more kinds of pathological changes.
- **Full set of CHASE-DB1** [13]: the images are captured by another type of fundus machine which has a smaller field of view.

From the evaluation results shown in Table 1, we can observe that: 1) BS+CWRGC+CWRVA achieves the best results in all datasets; 2) BS+CWRGC and BS+CWRVA outperform BS, BS+RGN and BS+SVGC in all datasets. 3) BS performs worst on DRIVE, DRIVE-GRAY and CHASE-DB1, but outperforms BS+RGN in STARE; 4) the performance of BS+RGN and BS+SVGC degenerates significantly on STARE and CHASE-DB1; 5) although CWRVA works slightly better than CWRGC in the DRIVE testing set, such superiority fails to generalize to other datasets; 6) SVGC achieves the highest SE in all testing set, at the expense of getting a much lower SP when comparing to BS+CWRGC, BS+CWRVA, and BS+CWRGC+CWRVA. Fig. 2 shows some visual examples of the segmentation results. The results suggest that the proposed method possess the significant generalization improvement to samples captured by different camera systems and/or affected by diverse pathological changes.

¹ <https://github.com/PaddlePaddle/PaddleSeg>

Table 1. Performance comparison on three Datasets.

	Method	AUC	ACC	SP	SE	F1
DRIVE	BS	0.9755	0.9531	0.9750	0.8055	0.8126
	BS + RGN	0.9769	0.9531	0.9746	0.8088	0.8131
	BS + SVGC	0.9772	0.9540	0.9752	0.8108	0.8167
	BS + CWRGC	0.9777	0.9539	0.9744	0.8150	0.8174
	BS + CWRVA	0.9783	0.9545	0.9741	0.8225	0.8205
	BS + CWRGC + CWRVA	0.9788	0.9545	0.9741	0.8227	0.8209
STARE	BS	0.9287	0.9334	0.9512	0.7103	0.6699
	BS + RGN	0.9147	0.9556	0.9812	0.6157	0.6273
	BS + SVGC	0.9288	0.9602	0.9837	0.6500	0.6769
	BS + CWRGC	0.9892	0.9676	0.9738	0.8902	0.8056
	BS + CWRVA	0.9771	0.9665	0.9816	0.7711	0.7652
	BS + CWRGC + CWRVA	0.9893	0.9683	0.9745	0.8908	0.8082
CHASE-DBI	BS	0.8794	0.9344	0.9825	0.2989	0.3768
	BS + RGN	0.9165	0.9394	0.9715	0.5159	0.5279
	BS + SVGC	0.9258	0.9465	0.9893	0.3848	0.4841
	BS + CWRGC	0.9812	0.9623	0.9702	0.8565	0.7563
	BS + CWRVA	0.9555	0.9522	0.9772	0.6230	0.6385
	BS + CWRGC + CWRVA	0.9838	0.9612	0.9673	0.8818	0.7565

3.3 Robustness to Brightness, Contrast and Saturation

In order to investigate a model’s robustness more comprehensively, three image processing functions are introduced here to respectively adjust the brightness, contrast and saturation of a color fundus image. Let V be the input image in RGB space, $\mathbb{G}(V)$ be the function to convert the input image from RGB space to gray space, and $\mathbb{M}(V)$ be the mean function, the brightness jitter, contrast jitter and saturation jitter can then be defined, respectively, as

$$\mathbb{B}(V) = V \cdot (1 - b), \quad (6)$$

$$\mathbb{C}(V) = V \cdot (1 - c) + \mathbb{M}(\mathbb{G}(V)) \cdot c, \quad (7)$$

$$\mathbb{S}(V) = V \cdot (1 - s) + \mathbb{G}(V) \cdot s \quad (8)$$

where $b \in [-1, 1]$ is brightness jitter ratio, $c \in [-1, 1]$ is the contrast jitter ratio, and $s \in [-1, 1]$ is saturation jitter ratio. The output values of these functions are all limited to $[0, 255]$.

By respectively varying b , c and s from -0.5 to 0.5 with a step of 0.1, we construct 30 more datasets with different degree of brightness, contrast and saturation based on the testing set of DRIVE. The evaluation results of different data augmentation strategies on these datasets are shown in Fig. 3. It can be obviously seen that : 1) models trained with the proposed methods are less sensitive to the variations of image brightness, contrast and saturation than BS and BS+RGN in terms of all the five evaluation metrics; 2) BS+CWRGC+CWRVA

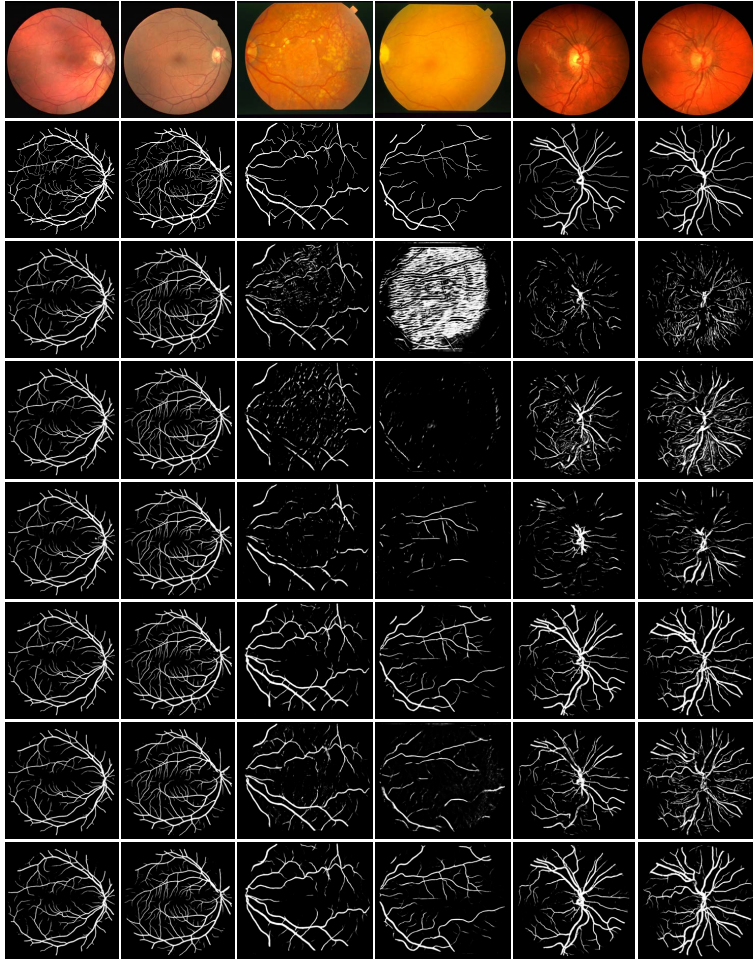


Fig. 2. Sample results on three different datasets. From up to bottom: input image, ground truth and predictive results of BS, BS+RGN, BS+SVGC, BS+CWRGC, BS+CWRVA, and BS+CWRGC+CWRVA. From left to right: sample images from DRIVE, DRIVE, STARE, STARE, CHASE-DB1, CHASE-DB1.

method consistently achieves the best results for all sorts of settings. These results indicate that the proposed method is less sensitive to the variations of image brightness, contrast and saturation.

4 Conclusion

This paper investigates the practicability and robustness of retinal vessel segmentation from a data augmentation perspective, with the advantages of not requiring extra training data or inference time. Our method comprises two new

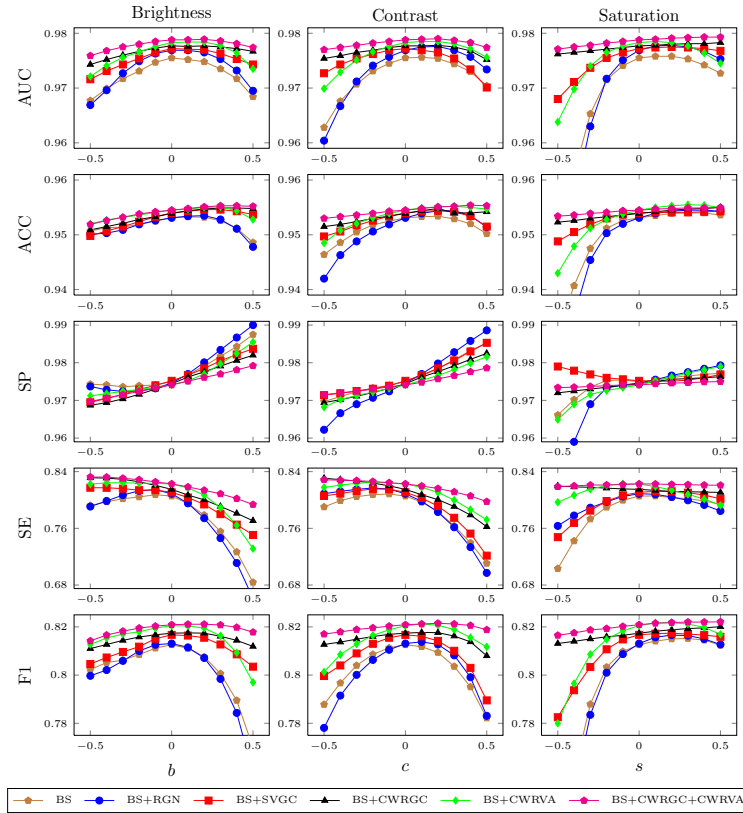


Fig. 3. Evaluation results to illustrate robustness of different methods to variations of brightness, contrast and saturation.

data augmentation modules to increase the performance and robustness of models learned. The channel-wise random gamma correction module aims at covering a wide range of tonal quality of the global image, while the channel-wise random vessel augmentation module focuses on diversifying the local visual appearance of the retinal vessels. The proposed methods achieve excellent results on both real-world and virtual datasets. Experimental results on various real-world public datasets show that the proposed method could consistently stabilize the segmentation performance on samples captured by different cameras or affected by various pathological changes. Moreover, by conducting synthetic databases, we also observe that the proposed method is less sensitive to the variations of image brightness, contrast, and saturation. Since robustness is an elementary requirement for almost all real world image analyzing systems, it remains an open question that if the proposed augmentation modules are also applicable for a wider range of computer vision tasks.

References

1. Araújo, R.J., Cardoso, J.S., Oliveira, H.P.: A deep learning design for improving topology coherence in blood vessel segmentation. In: International Conference on Medical Image Computing and Computer-Assisted Intervention. pp. 93–101. Springer (2019)
2. Bankhead, P., Scholfield, C.N., McGeown, J.G., Curtis, T.M.: Fast retinal vessel detection and measurement using wavelets and edge location refinement. *PloS one* 7(3) (2012)
3. Fan, Z., Lu, J., Wei, C., Huang, H., Cai, X., Chen, X.: A hierarchical image matting model for blood vessel segmentation in fundus images. *IEEE Transactions on Image Processing* 28(5), 2367–2377 (2018)
4. Fraz, M.M., Remagnino, P., Hoppe, A., Uyyanonvara, B., Rudnicka, A.R., Owen, C.G., Barman, S.A.: An ensemble classification-based approach applied to retinal blood vessel segmentation. *IEEE Transactions on Biomedical Engineering* 59(9), 2538–2548 (2012)
5. Fu, H., Xu, Y., Lin, S., Wong, D.W.K., Liu, J.: Deepvessel: Retinal vessel segmentation via deep learning and conditional random field. In: International conference on medical image computing and computer-assisted intervention. pp. 132–139. Springer (2016)
6. Gu, Z., Cheng, J., Fu, H., Zhou, K., Hao, H., Zhao, Y., Zhang, T., Gao, S., Liu, J.: Ce-net: context encoder network for 2d medical image segmentation. *IEEE transactions on medical imaging* 38(10), 2281–2292 (2019)
7. Hoover, A., Kouznetsova, V., Goldbaum, M.: Locating blood vessels in retinal images by piecewise threshold probing of a matched filter response. *IEEE Transactions on Medical imaging* 19(3), 203–210 (2000)
8. Japkowicz, N., Shah, M.: Evaluating learning algorithms: a classification perspective. Cambridge University Press (2011)
9. Javanmardi, M., Tasdizen, T.: Domain adaptation for biomedical image segmentation using adversarial training. In: 2018 IEEE 15th International Symposium on Biomedical Imaging (ISBI 2018). pp. 554–558. IEEE (2018)
10. Kanski, J.J., Bowling, B.: Clinical ophthalmology: a systematic approach. Elsevier Health Sciences (2011)
11. Leandro, J.J., Cesar, J., Jelinek, H.F.: Blood vessels segmentation in retina: Preliminary assessment of the mathematical morphology and of the wavelet transform techniques. In: Proceedings XIV Brazilian Symposium on Computer Graphics and Image Processing. pp. 84–90. IEEE (2001)
12. Liskowski, P., Krawiec, K.: Segmenting retinal blood vessels with deep neural networks. *IEEE transactions on medical imaging* 35(11), 2369–2380 (2016)
13. Owen, C.G., Rudnicka, A.R., Mullen, R., Barman, S.A., Monekosso, D., Whincup, P.H., Ng, J., Paterson, C.: Measuring retinal vessel tortuosity in 10-year-old children: validation of the computer-assisted image analysis of the retina (caiar) program. *Investigative ophthalmology & visual science* 50(5), 2004–2010 (2009)
14. Ronneberger, O., Fischer, P., Brox, T.: U-net: Convolutional networks for biomedical image segmentation. In: International Conference on Medical image computing and computer-assisted intervention. pp. 234–241. Springer (2015)
15. Soares, J.V., Leandro, J.J., Cesar, R.M., Jelinek, H.F., Cree, M.J.: Retinal vessel segmentation using the 2-d gabor wavelet and supervised classification. *IEEE Transactions on medical Imaging* 25(9), 1214–1222 (2006)

16. Staal, J., Abràmoff, M.D., Niemeijer, M., Viergever, M.A., Van Ginneken, B.: Ridge-based vessel segmentation in color images of the retina. *IEEE transactions on medical imaging* 23(4), 501–509 (2004)
17. Tyler, M.E., Hubbard, L., Boydston, K., Pugliese, A.: Characteristics of digital fundus camera systems affecting tonal resolution in color retinal images. *The Journal of Ophthalmic Photography* 31(1), 1–9 (2009)
18. Wang, B., Qiu, S., He, H.: Dual encoding u-net for retinal vessel segmentation. In: *International Conference on Medical Image Computing and Computer-Assisted Intervention*. pp. 84–92. Springer (2019)
19. Zhang, S., Fu, H., Yan, Y., Zhang, Y., Wu, Q., Yang, M., Tan, M., Xu, Y.: Attention guided network for retinal image segmentation. In: *International Conference on Medical Image Computing and Computer-Assisted Intervention*. pp. 797–805. Springer (2019)
20. Zhou, M., Jin, K., Wang, S., Ye, J., Qian, D.: Color retinal image enhancement based on luminosity and contrast adjustment. *IEEE Transactions on Biomedical Engineering* 65(3), 521–527 (2017)
21. Zhuang, J., Chen, Z., Zhang, J., Zhang, D., Cai, Z.: Domain adaptation for retinal vessel segmentation using asymmetrical maximum classifier discrepancy. In: *Proceedings of the ACM Turing Celebration Conference-China*. pp. 1–6 (2019)